



Universiteit  
Leiden  
The Netherlands

## **Towards a single-molecule FRET study of Frauenfelder's nonexponential rebinding of CO in myoglobin**

Eskandari Alughare, Z.

### **Citation**

Eskandari Alughare, Z. (2022, June 23). *Towards a single-molecule FRET study of Frauenfelder's nonexponential rebinding of CO in myoglobin*. *Casimir PhD Series*. Retrieved from <https://hdl.handle.net/1887/3348505>

Version: Publisher's Version

License: [Licence agreement concerning inclusion of doctoral thesis in the Institutional Repository of the University of Leiden](#)

Downloaded from: <https://hdl.handle.net/1887/3348505>

**Note:** To cite this publication please use the final published version (if applicable).

# 3

## Estimation of the dissociation quantum yield of the Mb-CO bond

*In this chapter, we describe experiments to estimate the quantum yield of MbCO dissociation using far red illumination in order to determine if that region can be used for an FRET experiments. The aim of Chapter 3 and 4 is to show that the rebinding of CO to protein at the single-molecule level can be done by performing single molecule-FRET experiments. In Chapter 3, we propose an approach using the weak bands beyond 700 nm in the deoxy-Mb absorption spectrum to quench the fluorescence of a deep red dye. Crucially, these bands are absent in the spectrum of MbCO, preventing breakage of the CO bond due to resonant energy transfer from the excited dye. As the different states of Mb can be readily distinguished by their UV/Vis spectra, this method was selected to determine the dissociation quantum yield.*

### 3.1 Introduction

In order to detect the activity of proteins, fluorescence spectroscopy is a reliable detection method. For example, azurin is a metalloprotein containing a copper center that can actively participate in electron transfer reactions. This copper site determines the redox property of azurin. The oxidized copper site ( $\text{Cu}^{2+}$ ) has a specific absorption spectrum in the area of 590-650 nm originating from  $\pi \rightarrow \pi^*$  transitions (Figure 3.1A). When the redox state of the prosthetic group switches to another state ( $\text{Cu}^{2+} \leftrightarrow \text{Cu}^+$ ) absorption in the visible part of the spectrum disappears. Because of the weakness of absorption spectrum for the oxidized copper site ( $\text{Cu}^{2+}$ ) in the area of 590-650 nm, it is difficult to follow the change of the oxidation state of Cu in azurin by monitoring the change of absorption spectra. However, this change on the absorption spectrum is key to monitoring the oxidation state of azurin by fluorescence spectroscopy. For example, attachment of a fluorescent molecule to the protein surface at a specific distance makes it possible to monitor the fluorescence emission of a single-dye-labeled azurin molecule by means of Förster Resonance Energy Transfer (FRET).<sup>1</sup> In fact, the oxidized form of azurin has more overlap with the emission spectra of a dye (for example Atto 655) compared to the reduced form of azurin, thus more fluorescence quenching is monitored due to the energy transfer from the labeled dye to the Cu-center (Figure 3.1B).<sup>2</sup>

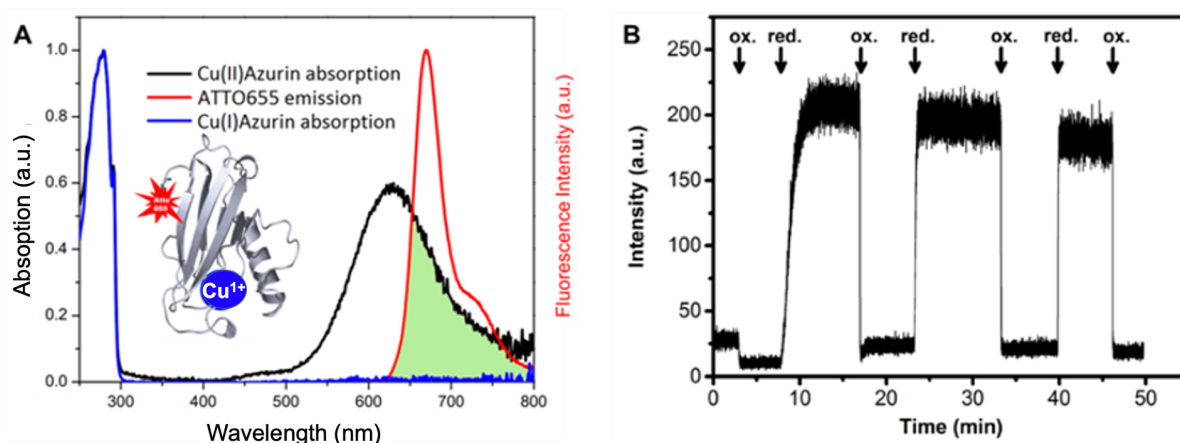


**Figure 3.1** (A) Absorption spectrum (black curve) of the oxidized form of azurin ( $\text{Cu}^{2+}$ ), emission spectra of Atto 655 dye (red curve), and the green colour area is a visualization of the overlap between the absorption spectrum of the oxidized form of azurin ( $\text{Cu}^{2+}$ ) and the emission spectrum of Atto 655 (B) The fluorescence intensity of azurin labeled with Atto 655 in solution (25 nM), the oxidized state ( $\text{Cu}^{2+}$ ) is quenched due to FRET and the reduced state ( $\text{Cu}^{1+}$ ) has high fluorescence intensity of the Atto655 dye due to the absence of FRET.<sup>2</sup>

In the same way, we will explore the use of FRET to monitor the kinetics of rebinding of small molecules to proteins. For example, myoglobin is another metalloprotein (Mb) that has been used as a model system for many experiments, particularly for kinetics-structural relationships. It has a heme containing an iron reaction center that can bind to small ligands such as  $\text{O}_2$ , CO, or NO reversibly.

In the case of myoglobin, the binding or unbinding of CO ligand to the heme reaction center gives rise to a different absorption spectrum (Figure 3.2). Thus, by labeling myoglobin with a proper dye, the overlap between the emission spectrum of the dye-labeled myoglobin with the absorption spectrum of these different states (with bound

or unbound CO) is changed and, due to the different FRET efficiency, it is possible to study the CO binding and rebinding kinetics. When the CO molecule in the heme pocket of myoglobin dissociates, the fluorescence intensity of the dye attached to the MbCO is quenched due to the stronger energy transfer from the dye label to the heme center of deoxy-Mb (Figure 3.3).

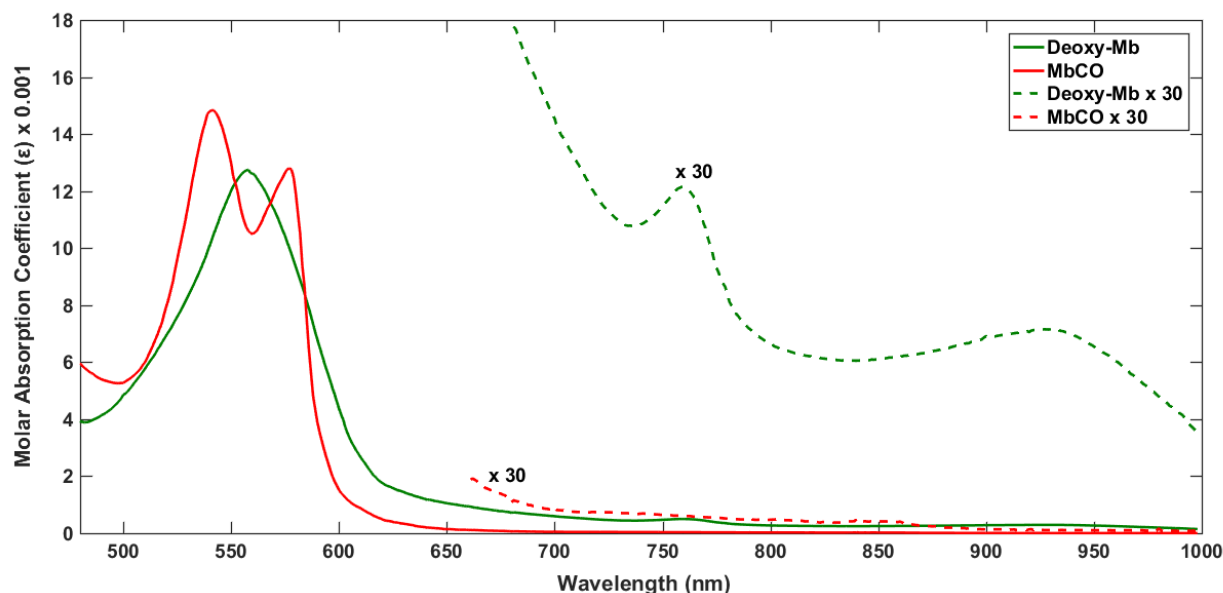


**Figure 3.2** Absorption spectrum of the Q-bands (500-700 nm) and NIR bands (700-1000 nm) for two Mb states: deoxy-Mb (green), and MbCO (red) from horse heart Mb at room temperature, in Sørensen's phosphate buffer (0.05 mM) with pH 6.8-8. The dashed lines represent the 30x enlarged spectra. <sup>3</sup>

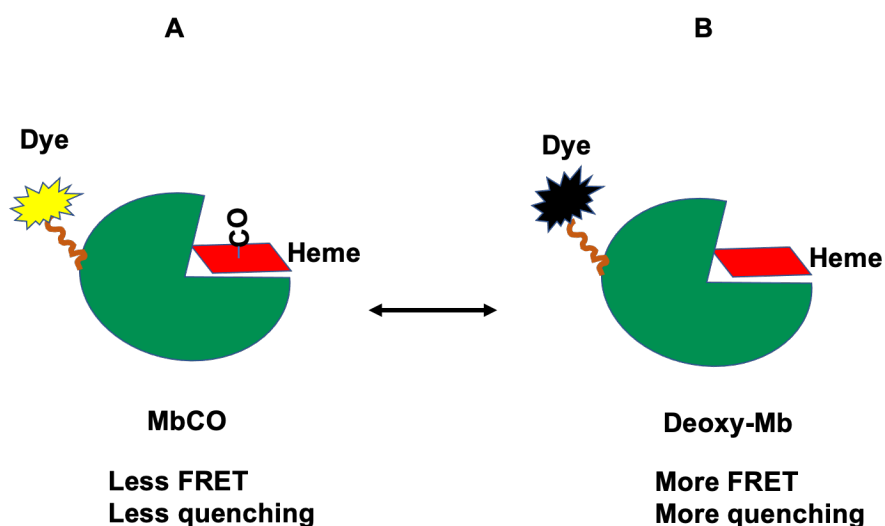


**Figure 3.3** A schematic illustration of MbCO containing CO bound to the heme (red) (A), and deoxy-Mb in which CO is unbound to the heme (B). The fluorescence intensity of a suitable dye attached to MbCO is quenched due to stronger FRET when the CO molecule detaches from the heme, due to energy transfer to the heme center of deoxy-Mb.

The single-molecule FRET (smFRET) approach has been widely used to determine kinetic rates of protein reactions. Proteins can be specifically labeled by a dye enabling

smFRET measurements. The ability to measure accurate distances and kinetics with smFRET enables studies of dynamics and structural biology and monitoring the biomolecular heterogeneities through the behavior of individual molecules.<sup>1</sup>

#### 3.1.1 Does near infra-red light ( $\lambda > 700$ nm) break the Mb-CO bond?

It is well known that a wide spectral range of visible light, particularly  $400 < \lambda < 550$  nm, breaks the Mb-CO bond with high efficiency, which precludes using FRET-based investigations of CO dissociation in this spectral region. We therefore investigated a strategy involving the near infra-red spectral region,  $\lambda > 700$  nm. If a labeled MbCO under red-light illumination breaks the Mb-CO with high efficiency, probing the absorption of MbCO with red light would dissociate the complex to regenerate deoxy-Mb, making it difficult to monitor CO rebinding by fluorescence spectroscopy using FRET spectroscopy. For this reason, it is essential to estimate the quantum yield for photodissociation of the Mb-CO bond under red-light illumination.

As discussed in Chapter 2, the myoglobin spectrum can be broadly split into three regions: the Soret band (300-500 nm), the Q-bands (500-700 nm) and the NIR bands I, II, and III (700-1000 nm) (Figure 3.4). The quantum yield of Mb-CO bond breaking is close to unity when under illumination by light with a wavelength shorter than 600 nm, but it is still unknown whether illumination with  $\lambda > 700$  nm (Figure 1) breaks the MbCO bond, and with which quantum yield. In this chapter, we report our measurements of the dissociation quantum yield of Mb-CO in the near infra-red.

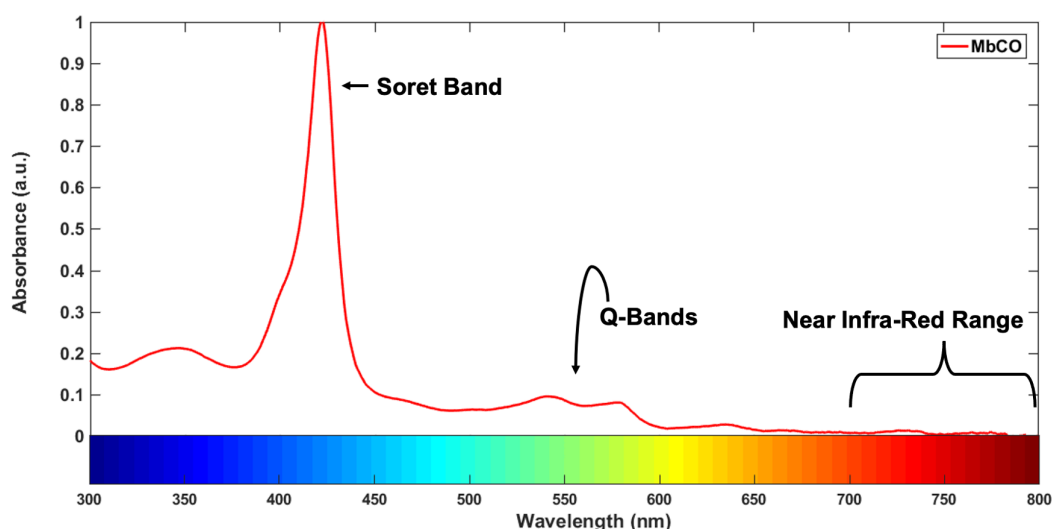


**Figure 3.4** Absorption spectrum of MbCO from the uV to the near infra-red

If the quantum yield in this far-red area would be significantly less than 1, it might be possible to detect the signal of the dye label emitting in the far red (700-1000 nm). It would thus enable us to distinguish between the carboxy and deoxy forms and thereby to monitor the kinetics of the CO rebinding to a single myoglobin molecule. In this chapter, we focus on ensemble experiments only.

#### 3.1.2 Preparation of MbCO and deoxy-Mb from Met-Mb

The first step is the preparation of MbCO from the commercially available form of myoglobin, met-Mb, in which the heme contains the ferric iron ( $\text{Fe}^{3+}$ ). Met-Mb ( $\text{Fe}^{3+}$ ) is

reduced to the deoxy form in which the iron is in the  $\text{Fe}^{2+}$  oxidation state. Incubation with CO then yields MbCO (Figure 3.5).

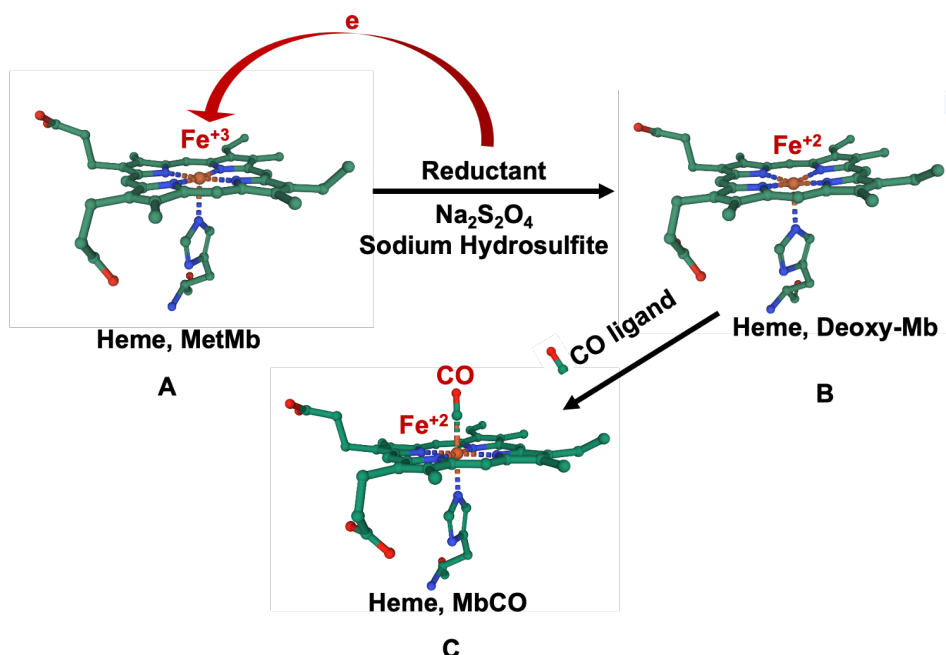


**Figure 3.5** Schematics of MbCO preparation from met-Mb. (A) The heme in met-Mb is reduced with sodium hydrosulfite, making (B) deoxy-mb with ferrous iron. (C) Incubation with CO yields MbCO. The images of hemes have been exported from the PDB (Horse heart 1WLA, 5D5R, and 1A6G for met-Mb, deoxy-Mb, and MbCO respectively)

### 3.1.3 Photodissociation methods

The three standard methods for the measurement of ligand photolysis are: (i) the kinetic method, (ii) the steady-state method, and (iii) the pulse photolysis method. The first two focus on bimolecular rebinding and use constant illumination so that either the rates of transition between the photostationary states, or the equilibrium ligand binding curves are measured. The measured rate is the sum of the association and dissociation rates and the yield is the overall “bimolecular dissociation yield”. The pulse photodissociation method relates to the rebinding kinetics and utilizes a pulse that is short compared to the ligand recombination time. Pulse widths in the millisecond to microsecond range are sufficient to measure bimolecular dissociation yields. Studies with nanosecond or faster time resolution found that a photodissociated ligand can remain in the heme pocket and recombine geminately. The bimolecular dissociation yield is then expressed as  $\eta_b = Y\eta_0$ , where  $\eta_0$  is the ( $t = 0$ ) photodissociation yield (sometimes referred to as the intrinsic quantum yield of photodissociation) and  $Y$  is the fraction of ligands that escape to the solution and do not undergo geminate rebinding. As the different states of Mb can be readily distinguished by their UV/Vis spectra, UV-Vis spectroscopy was selected to measure the dissociation rate of MbCO and to determine the dissociation quantum yield.

## 3.2 Results

### 3.2.1 Preparation of deoxy-Mb and MbCO from met-Mb

To reduce met-Mb to deoxy-Mb, it is important to prepare the sample in an oxygen-free environment. Therefore, first, the met-Mb solution was degassed in an absorption cell (cuvette). In this study, two different methods have been tested to prepare an oxygen-free solution and to prepare deoxy-Mb and MbCO: glass-apparatus and the nitrogen-box.

The home-made glass apparatus is shown in Figure 3.6. The sample cell was connected to a glass setup (Figure 3.6 B, and C) to remove oxygen by alternating N<sub>2</sub> bubbling and evacuating during 10 min. Sodium hydrosulfite crystals (sodium dithiote, DTT) as reducing agent were placed in a side arm of a modified glass tube (Figure 3.6 A) and phosphate buffer was added to the mixing chamber. The modified glass tube was connected to the same glass setup the buffer was degassed and the glass were tilted to add the sodium hydrosulfite in the side arm to the solution, producing an oxygen-free sodium hydrosulfite reducing agent. Using a Hamilton syringe, the reducing solution of sodium hydrosulfite was transferred anaerobically to the met-Mb absorption cell to produce deoxy-Mb. MbCO was prepared by a similar treatment starting from deoxy-Mb, omitting the addition of the reducing agent and replacing N<sub>2</sub> with CO.

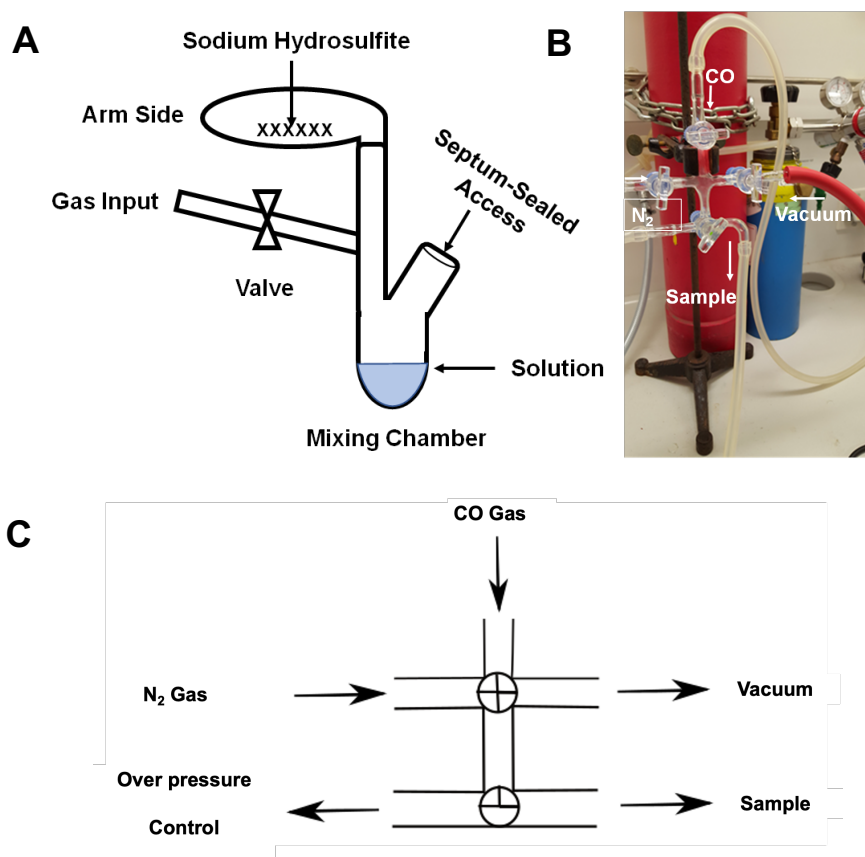


**Figure 3.6** Scheme of setup for preparation of deoxy-Mb and MbCO; (A) Modified glass tube for met-Mb reduction shows the side arm, gas input, valve, mixing chamber and septum-sealed access, (B) CO gas setup, (C) Sketch of CO gas setup shows the CO and N<sub>2</sub> gas entrances, vacuum, sample position, and N<sub>2</sub> overpressure control.



The second method to prepare deoxy-Mb and MbCO samples consists of bubbling the buffer solution with  $N_2$  inside a cuvette sealed with a septum, using nitrogen from a gas cylinder and then performing the reactions inside a nitrogen-filled dry box. Dissolving met-Mb in the buffer results in a brown-colored solution (Figure 3.7, A). Met-Mb is then reacted with DTT in an oxygen-free atmosphere producing deoxy-Mb with a purple color (Figure 3.7, B). Then bubbling the solution in the cuvette with CO from a Minican for 10 min converts deoxy-Mb to MbCO resulting in a red-colored solution (Figure 3.7, C).

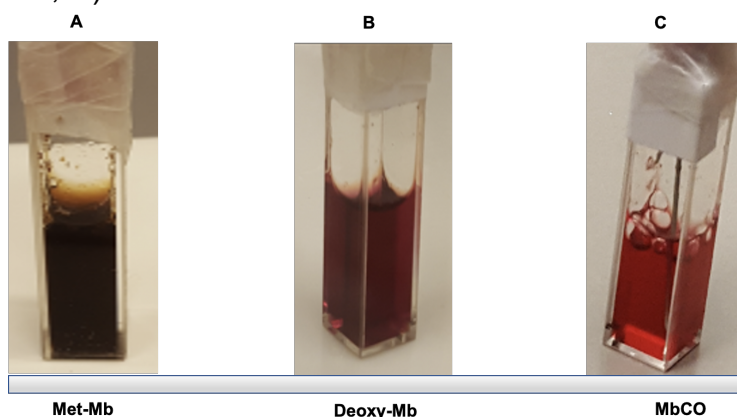


**Figure 3.7** The sealed cuvette. (A) brown solution of met-Mb, (B) deoxy-Mb solution with purple color, and (C) MbCO solution with red color.

Both methods produced pure MbCO samples but the second procedure is more straightforward and safer although it takes more time. All MbCO used in the experiments in this chapter was prepared using the nitrogen box system.

The changes in absorption spectra (Chapter 2, section 2.1) of Mb can be used to determine the state of the myoglobin present in the solution. The successful preparation of deoxy-Mb and MbCO was verified by measuring the absorption spectra with a UV-Vis spectrophotometer (Figures 3.8 and 3.9). It should be noted that because of the low extinction coefficient of band III in deoxy-Mb, it was only observed at high concentrations of deoxy-Mb (1 mM).

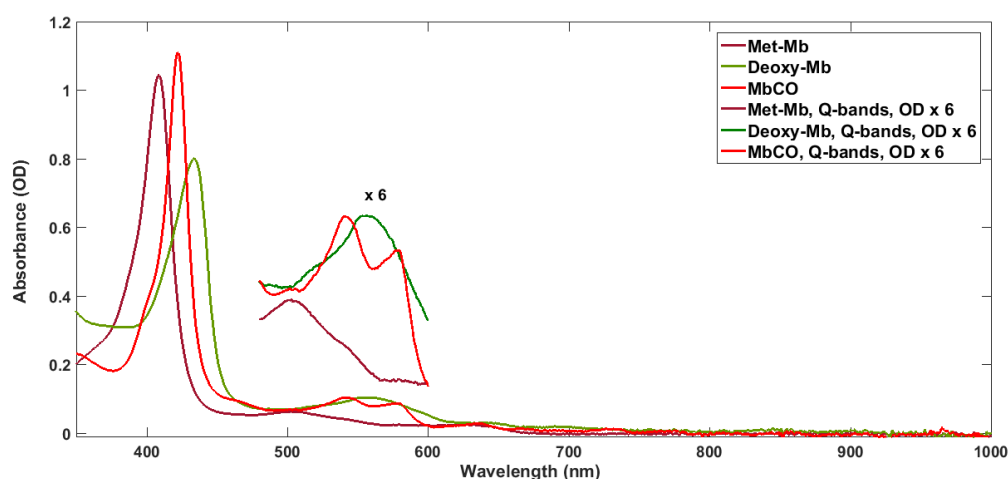


**Figure 3.8** Absorption spectrum of met-Mb (brown) (Soret band at 409 nm), deoxy-Mb (green) (Soret band at 433 nm), and MbCO (red) (Soret band at 423 nm). These spectra all are results of our experiments.



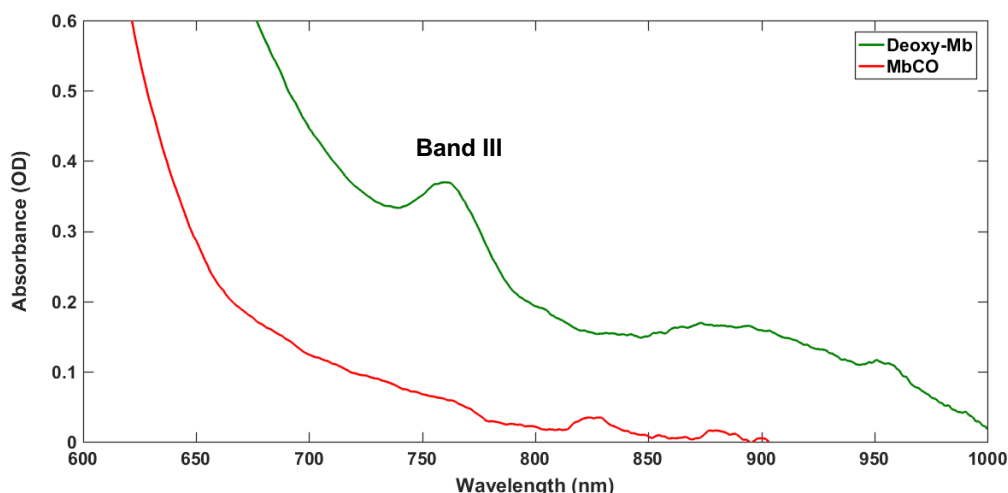


**Figure 3.9** Absorption spectra of 1mM deoxy-Mb (blue) (Band III occurs at 760 nm) and MbCO (red) (1mM) in PBS, pH=7.2, at room temperature. These spectra are the results of our experiments.

#### 3.2.2 Design of the setup

To study the photodissociation kinetics of Mb-CO, a UV-Vis cell holder was used consisting of a cuvette, a blue or red filter, and blue or near infra-red LEDs. This cell allows for illumination inside the UV-Vis spectrometer with high illumination efficiency of the sample. The cell allows the use of the UV-Vis spectrometer to measure the absorption spectrum of the solution in the cuvette and to follow the kinetics of dissociation/rebinding (Figure 3.10).

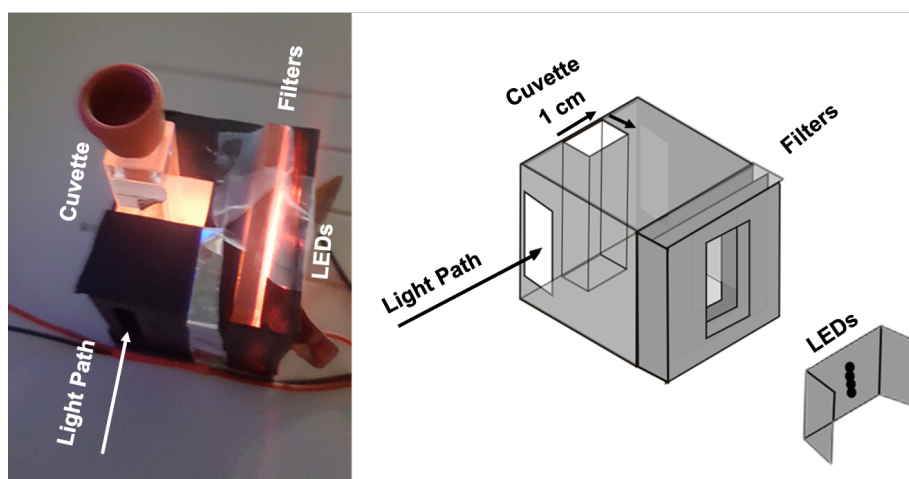


**Figure 3.10** The UV-Vis sample holder consists of a cuvette positioner, filters, a LED holder. The light path of the spectrophotometer is indicated. Irradiation of the sample in the cuvette by LED light follows a perpendicular path.

#### 3.2.3 Study of photodissociation kinetics of Mb-CO and designed experiment

The geminate rebinding of photodissociated CO in the vicinity of the heme at room temperature is fast compared to the recombination of CO from solution to the heme. Therefore, we ignore the geminate rebinding and only focus on the recombination of

CO from solution to the heme pocket. To study the kinetics of MbCO photodissociation, it is essential to slow down the recombination kinetics of the escaped CO molecule in solution to the heme. In this regard, CO molecules after escaping from the protein should be removed from the vicinity of the formed deoxy-Mb. In our first attempts, pure nitrogen gas was bubbled during illumination to remove any dissociated CO near the myoglobin protein. It appeared that even removing of CO molecule in solution during photodissociation by bubbling pure nitrogen gas does not completely prevent the recombination of CO that has escaped to the solution. Moreover, bubbling nitrogen gas removed some amount of protein from the detection area and caused an error in the measurement of absorption spectra. Alternatively, the bubbling may have caused denaturation of some of the protein during the experiment. A different approach to prevent CO recombination to the heme is to control this reaction chemically. During photodissociation of MbCO, deoxy-Mb is formed. Thus if an oxidant with a fast rate converts the deoxy-Mb to another form, for example met-Mb, not only is the recombination reaction prevented, but we also reach a simpler mixture solution after illumination, which facilitates the determination of the exact amount of MbCO converted to deoxy-Mb. We can thus more easily calculate the photodissociation quantum yield of MbCO with red-LED illumination by comparing it to that with blue-LED illumination measured in a control experiment.  $\text{H}_2\text{O}_2$  is an oxidant which is small enough to enter the iron cavity in the protein and to convert deoxy-Mb (containing iron (II)) by supplying an electron to met-Mb (containing iron (III)) (Figure 3.11 B,  $B \rightarrow C$ ).

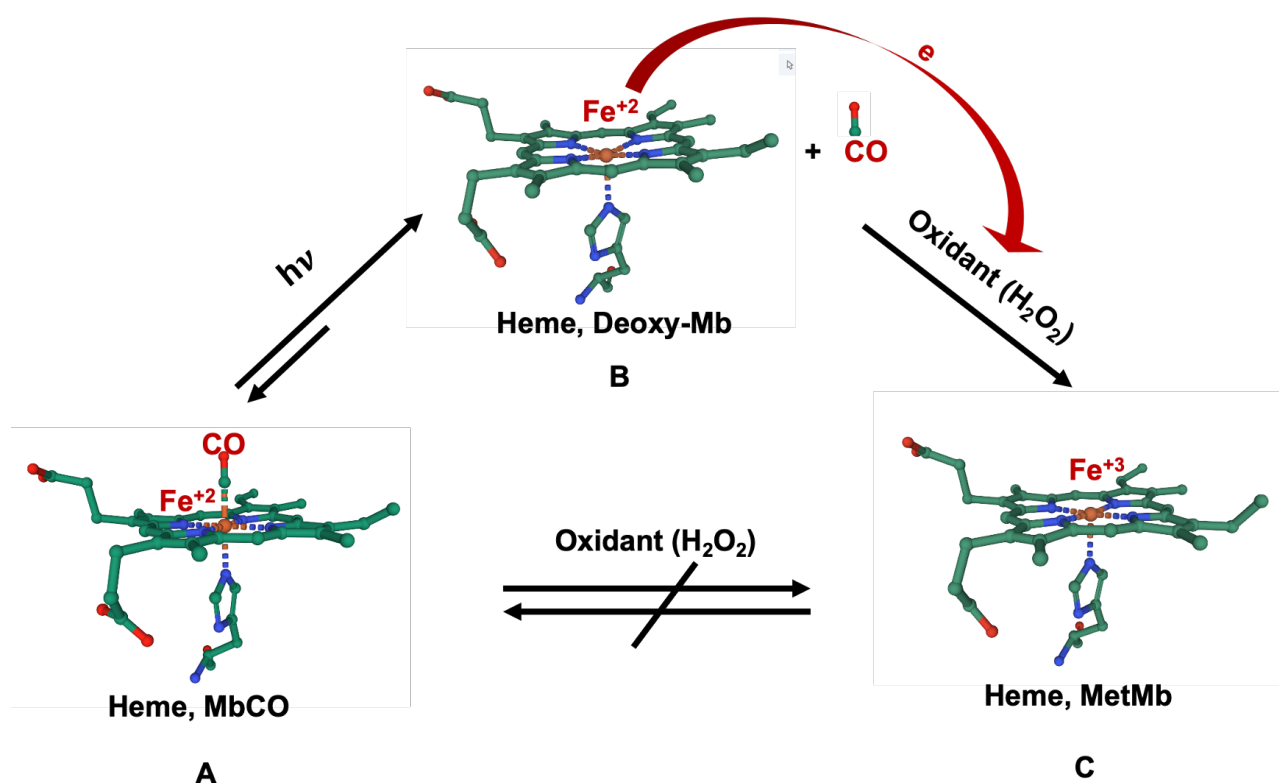


**Figure 3.11** A schematics of the experimental design to measure the quantum yield of MbCO photodissociation (A) MbCO is photodissociated to deoxy-Mb ( $A \leftrightarrow B$ ), (B) The heme in deoxy-Mb is oxidized with  $\text{H}_2\text{O}_2$  ( $B \leftrightarrow C$ ), (C) Met-Mb and MbCO do not convert to each other in presence of  $\text{H}_2\text{O}_2$  (A, C). The images of hemes have been exported from PDB (The Horse heart 1A6G, 5D5R, and 1WLA for MbCO, deoxy-Mb, and met-Mb respectively)

### 3.2.4 Control experiment

We want to be sure that in the following MbCO photodissociation experiments under oxidizing conditions, MbCO itself is not oxidized by  $\text{H}_2\text{O}_2$  (Figures 3.11 C, and 3.12) and only deoxy-Mb (the product of Mb-CO dissociation) reacts with  $\text{H}_2\text{O}_2$  and produces met-Mb (Figure 3.11 A).

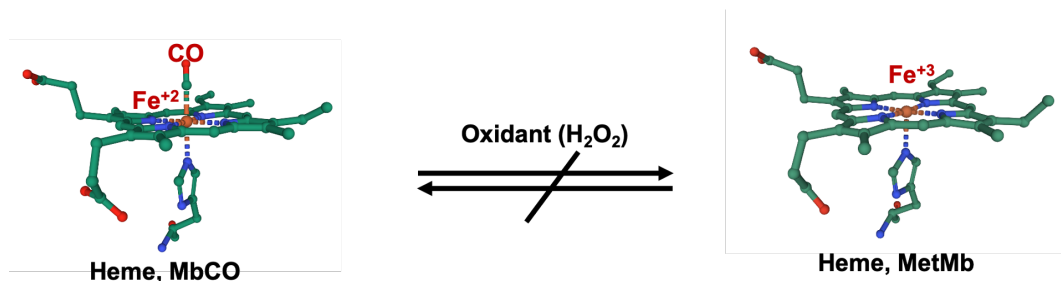


**Figure 3.12** A schematics of control experiment. MbCO does not convert to met-Mb, even in the presence of  $\text{H}_2\text{O}_2$ , and the inverse reaction doesn't occur either. The images of the heme groups have been exported from the PDB (Horse heart 1A6G, and 1WLA for MbCO, and met-Mb respectively)

As a control experiment, the absorption spectrum of MbCO in the presence of oxidant ( $\text{H}_2\text{O}_2$ ) without illumination was followed over time to check for any possible changes because of the presence of the oxidant (Figure 3.13). Before that, the excess of CO in the solution was removed by bubbling the sample with pure  $\text{N}_2$ .

As it can be seen in Figure 3.13, there is not any change in the absorption spectrum of MbCO mixed with  $\text{H}_2\text{O}_2$ , even in the presence of an excess of  $\text{H}_2\text{O}_2$  and after a long incubation time of 2 hours. It should be noted that met-Mb cannot be reduced in our oxidizing conditions. Therefore, the reverse reaction, the conversion of met-Mb to MbCO, cannot occur.

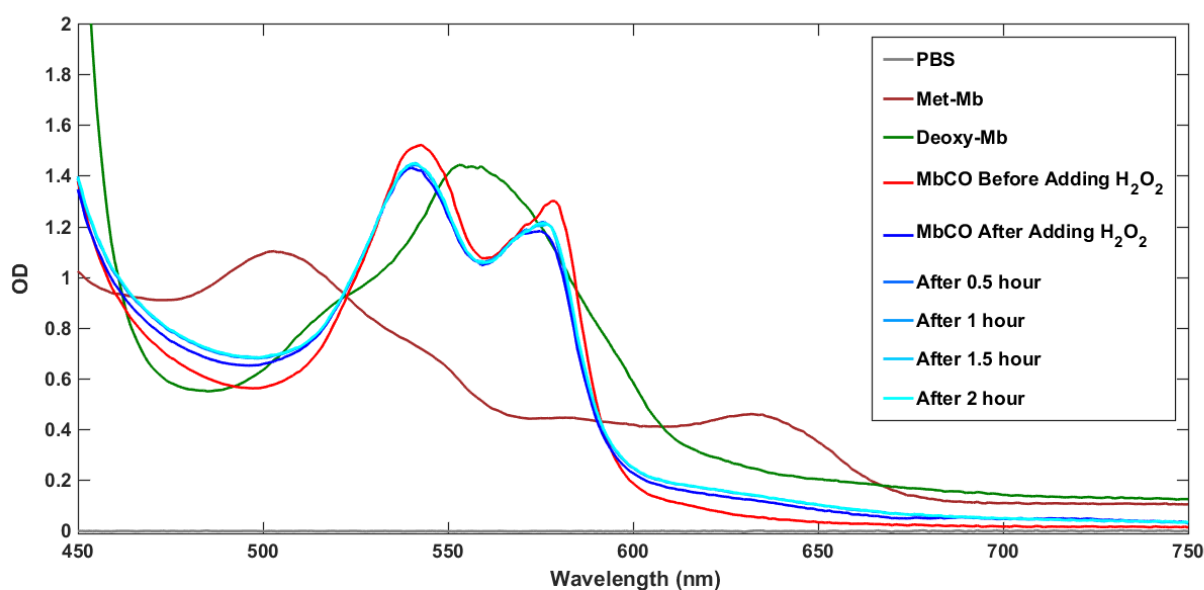


**Figure 3.13** Absorption spectra of MbCO before (red) and after adding an excess amount of oxidant ( $\text{H}_2\text{O}_2$ ) (dark blue) and followed over time (lighter blue) without illumination, in PBS,  $\text{pH}=7.2$ , at room temperature.

In our designed experiment (Figure 3.11) to calculate the quantum yield of MbCO photodissociation, it is essential that after each MbCO is dissociated with a photon and CO escapes to the solution, the deoxy-Mb is efficiently and quickly oxidized by  $\text{H}_2\text{O}_2$ , producing met-Mb with high yield, and also that the produced met-Mb should not revert back to deoxy-Mb (Figures 3.11 B, and 3.14). Therefore, by measuring the amount of met-Mb as a function of time, the quantum yield of Mb-CO bond breaking can be determined. Thus, the reaction of deoxy-Mb with  $\text{H}_2\text{O}_2$  was monitored by following the absorption spectra over time under our oxidizing conditions.

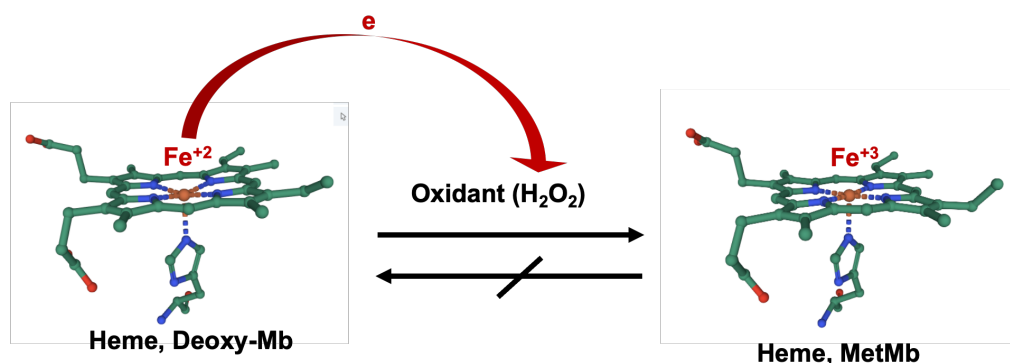


**Figure 3.14** A schematics of control experiment. Deoxy-Mb quickly converts to met-Mb in the presence of  $\text{H}_2\text{O}_2$ , whereas the reverse reaction is impossible. The images of hemes have been exported from the PDB (Horse heart 1A6G, and 1WLA for deoxy-Mb, and met-Mb respectively)

Figure 3.14 shows the schematic conversion of deoxy-Mb to met-Mb. It should be noted that some articles mention that met-Mb can convert to the intermediate named ferryl oxide in the presence of an excess (2 M) of  $\text{H}_2\text{O}_2$ .<sup>4</sup> Possible binding of oxygen from the solution to deoxy-Mb is of no concern, as it cannot displace CO. Figure 3.15 shows our measured absorption spectra of deoxy-Mb after adding an excess amount of oxidant ( $\text{H}_2\text{O}_2$ ), which yields a mixture of met-Mb and ferryl-Mb.

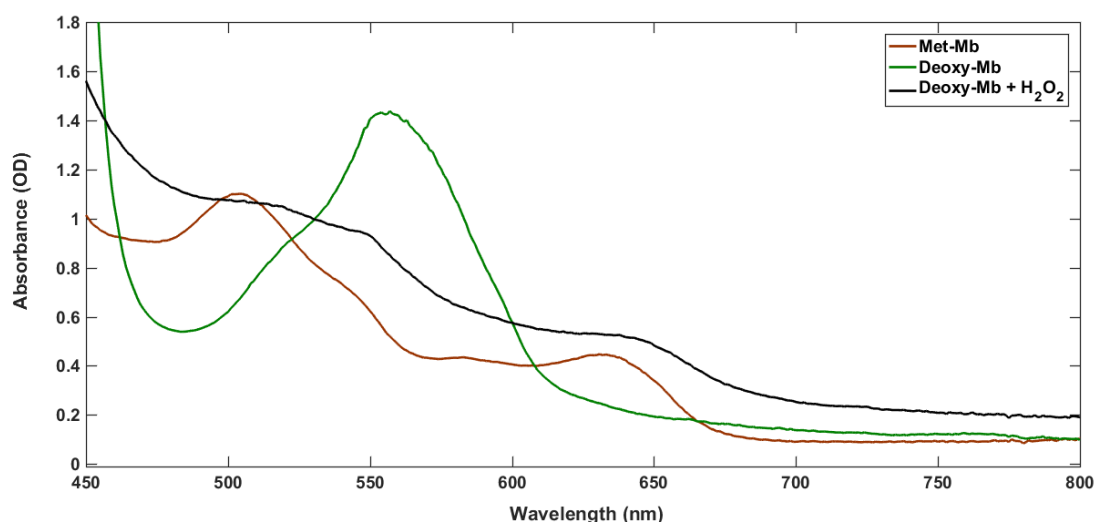


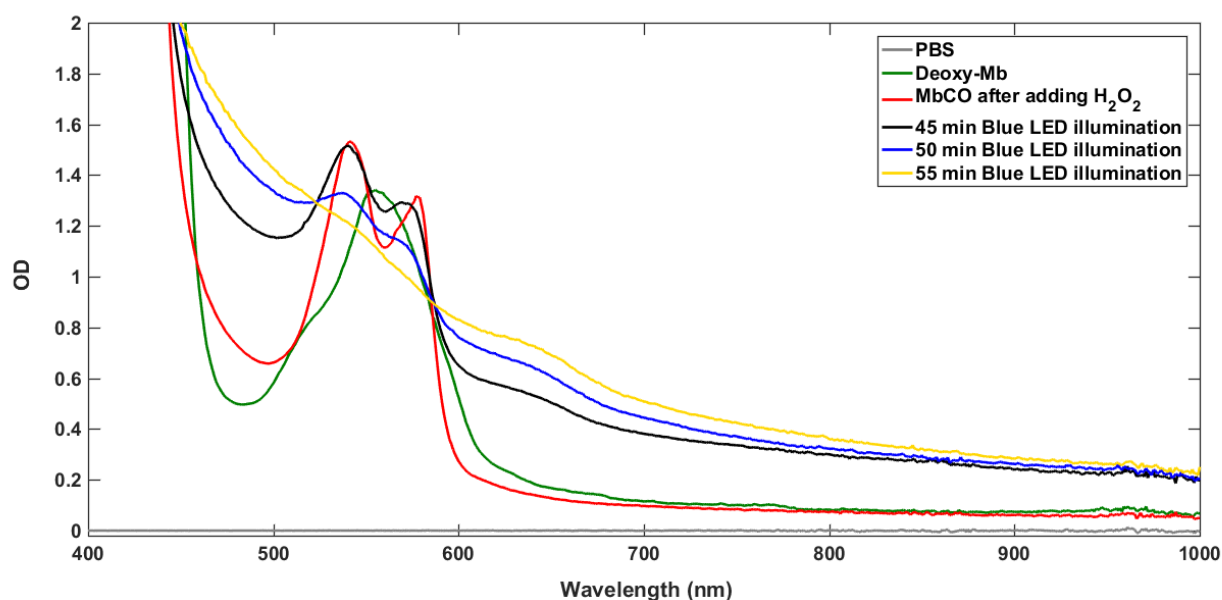
**Figure 3.15** Absorption spectra of met-Mb (brown), deoxy-Mb (green) and deoxy-Mb after adding an excess amount of oxidant ( $\text{H}_2\text{O}_2$ ) (black) in PBS, pH=7.2, at room temperature. Deoxy-Mb converts to a mixture of met-Mb and ferryl-Mb.<sup>4</sup>

### 3.2.5 Study of the photodissociation kinetics of Mb-CO in the presence of $\text{H}_2\text{O}_2$ under blue LED illumination ( $\lambda = 450 \text{ nm}$ )

As the quantum yield of MbCO bond breaking by blue light is close to 1, we can use this photoreaction as a reference. Photodissociation of MbCO will lead to deoxy-Mb, which under our oxidizing conditions will immediately be converted to met-Mb, enabling us to titrate the dissociated MbCO quantitatively. To study the photodissociation kinetics of MbCO, we illuminated the protein solution in the presence of oxidant using a near infra-red LED ( $\lambda = 730 \text{ nm}$ ) and the absorption at  $540 \text{ nm}$  (Q-band) was followed over time to measure the kinetics of the Mb-CO bond breaking. This experiment was repeated with blue LED light ( $\lambda = 450 \text{ nm}$ ) as a reference. Therefore, later we will compare illumination by blue light ( $\lambda = 450 \text{ nm}$ ) (reference experiment) with illumination by red light ( $\lambda = 730 \text{ nm}$ ), both in the presence of oxidant. One requirement to measure the quantum yield of the MbCO bond breaking is the precise determination of the excitation efficiencies at the emission wavelengths of the red and blue LEDs.

The LED experiments will be compared to a control experiment with no illumination to eliminate unknown factors that may influence the results of control and LED illumination experiments, provided these influences are identical (Figures 3.13).

The reference experiment includes 12 cycles of blue-light illumination of MbCO in the presence of oxidant,  $\text{H}_2\text{O}_2$ . The duration of each cycle is 5 minutes Blue LED illumination. After each cycle, the absorption spectrum of the sample was recorded while the blue LED was turned off. Figure 3.16 shows the absorption spectrum changes of MbCO under blue LED light ( $\lambda = 450 \text{ nm}$ ) over time.



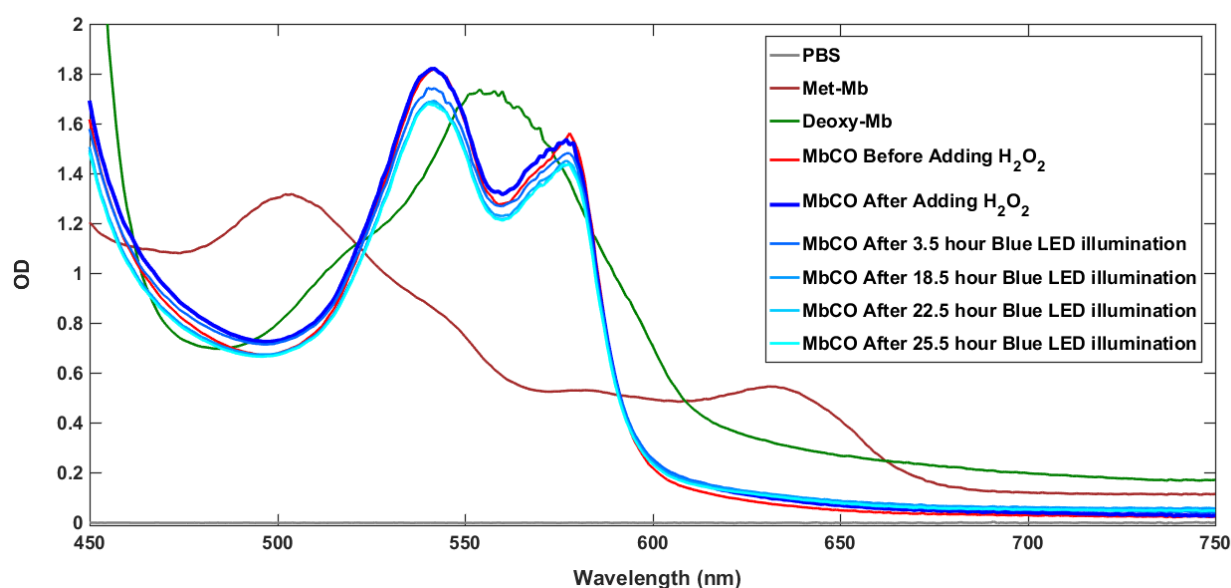
**Figure 3.16** Absorption spectra of MbCO in the presence of an excess amount of oxidant ( $\text{H}_2\text{O}_2$ ) (red) and after blue-light illumination ( $\lambda = 450 \text{ nm}$ ) over time at room temperature. Under blue-light illumination, MbCO dissociates to form deoxy-Mb, which immediately converts to met-Mb or ferryl forms.

Figure 3.16 clearly shows the change in the absorption spectrum in the Q-bands regions of MbCO before and after illumination with blue light. As can be seen, before illumination there are two peaks at 542 nm and 579 nm which are absorption characteristic for MbCO. After around 1 hour of illumination with blue light, they completely disappear. This is consistent with the conversion of MbCO to deoxy-Mb by blue light and full conversion of deoxy-Mb to met-Mb and ferryl forms.

Moreover, the rate of MbCO breaking is very fast and, after 60 min, a full conversion of MbCO to deoxy-Mb by blue-light illumination occurred, followed by the fast oxidation of deoxy-Mb to met-Mb by  $\text{H}_2\text{O}_2$ .

### 3.2.6 Study of photodissociation kinetics of the Mb-CO in the presence of $\text{H}_2\text{O}_2$ and near infra-red LED illumination ( $\lambda = 730 \text{ nm}$ )

To study photodissociation kinetics of MbCO in the near infra-red region, we illuminated a myoglobin solution containing an excess amount of oxidant ( $\text{H}_2\text{O}_2$ ) with near infra-red LED light ( $\lambda = 730 \text{ nm}$ ). The absorption at 540 nm (Q-band) was followed over time to measure the kinetics of the Mb-CO bond breaking. As can be seen in Figure 3.17, even over a long time (25.5 hours) no change in the absorption spectrum of MbCO was observed, which clearly shows that near infra-red LED light ( $\lambda = 730 \text{ nm}$ ) is much less efficient than blue light in breaking the MbCO bond. Figure 3.18 shows the change of the OD of MbCO solution at a wavelength 540 nm over time.



**Figure 3.17** The absorption spectra of MbCO before (red) and after adding an excess amount of oxidant ( $\text{H}_2\text{O}_2$ ) (dark blue) and following over time (lighter blue) under near infra-red LED illumination ( $\lambda = 730 \text{ nm}$ ) in PBS,  $\text{pH}=7.2$ , at room temperature.



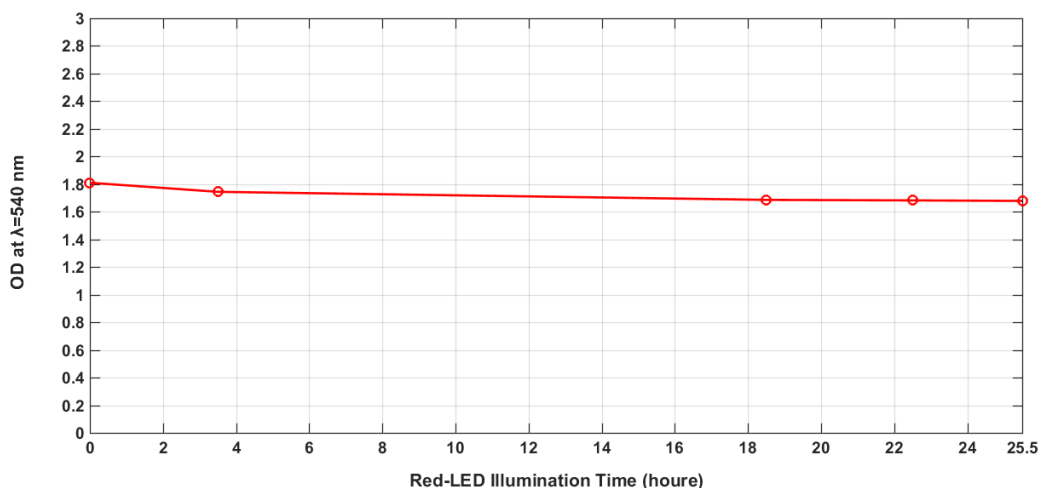


**Figure 3.18** The OD of a MbCO solution at wavelength 540 nm was measured after 3.5, 18.5, 22.5, and 25.5 hours) under near infra-red LED illumination ( $\lambda = 730$  nm) in PBS, pH=7.2, at room temperature.

#### 3.2.7 Estimation of photon rate

Another challenge is that MbCO has a very low absorbance in the near infra-red spectral region so the excitation efficiency is very low. To solve this problem, a highly efficient illumination is needed. Moreover, it is difficult to determine the excitation efficiency by the LEDs precisely. In addition, the possibility of CO rebinding may complicate the kinetics of rebinding.

To estimate the quantum yield, it is first necessary to determine the relative photon absorption rate of red versus blue photons. Here, the ( $t = 0$ ) photodissociation quantum yield ( $\eta_0$ ) of MbCO with the near infra-red LED ( $\lambda_{\max} = 730$  nm,  $\eta_0(R)$ ) is estimated compared to the photodissociation quantum yield of MbCO with blue LED ( $\lambda_{\max} = 450$  nm) which we assume is unity, ( $\eta_0(B) = 1$ ) taken as a reference.

The ratio of the number of Mb-CO bonds broken with near infra-red LED compared to blue LED can be calculated by the estimation of the probability of MbCO bond breaking (the efficiency of MbCO photodissociation), the probability of photon absorption photon and the number of absorbed photons by the MbCO molecules (eq 3.1).

$$\frac{N_{\text{broken bonds}}_{\text{-RED}}}{N_{\text{broken bonds}}_{\text{-BLUE}}} = \left( \frac{\eta_0(R)}{\eta_0(B)} \right) \cdot \left( \frac{N_{\text{Incident photon per second}}_{\text{-RED}}}{N_{\text{Incident photon per second}}_{\text{-BLUE}}} \right) \cdot \left( \frac{\text{Time Incident photon}_{\text{-RED}}}{\text{Time Incident photon}_{\text{-BLUE}}} \right) \cdot \left( \frac{P_{\text{Incident photon}}_{\text{-RED}}}{P_{\text{Incident photon}}_{\text{-BLUE}}} \right) \quad 3.1$$

The number of incident photons per second emitted from the near infra-red and blue LEDs are obtained by measuring the power of illumination light passing through the filters into the MbCO solution inside the cuvette, and by taking into account the energy of blue and red photons which have a different energy per photon. The power of blue



LED and near infra-red LED were measured to be 0.5, and 2 mW, respectively, with a photon energy ratio of 1.62. The ratio of the number of incident photons per second emitted from red and blue LEDs was calculated to be 6.48. Finally, the ratio of the numbers of incident photons over the whole duration of the experiments (25.5 hours for the near infra-red LED illumination and around 1 hour for the blue LED illumination) is 165.2.

The number of absorbed photons depends on three factors including the brightness of the LEDs, the transmission of excitation light through the filters between the LEDs and the samples, as well as the absorptivity of the MbCO molecules at the respective wavelengths. It should be noted that based ref. 3, the ratio of absorptivity of MbCO at 450 nm, and 730 nm is 82 ( $\frac{\epsilon_{730 \text{ nm}}}{\epsilon_{450 \text{ nm}}} = 82$ ). The number of absorbed photons was obtained by multiplying the LED intensity, the transmission of the filter used (see Figures 3.19, 3.20) and the absorbance of MbCO at each wavelength (Figure 3.21). Based on our calculation, the ratio of the numbers of absorbed photons for red to blue LED illumination is 0.0978.

The illumination efficiency of red to blue is calculated as 16.1 according to eq 3.1.

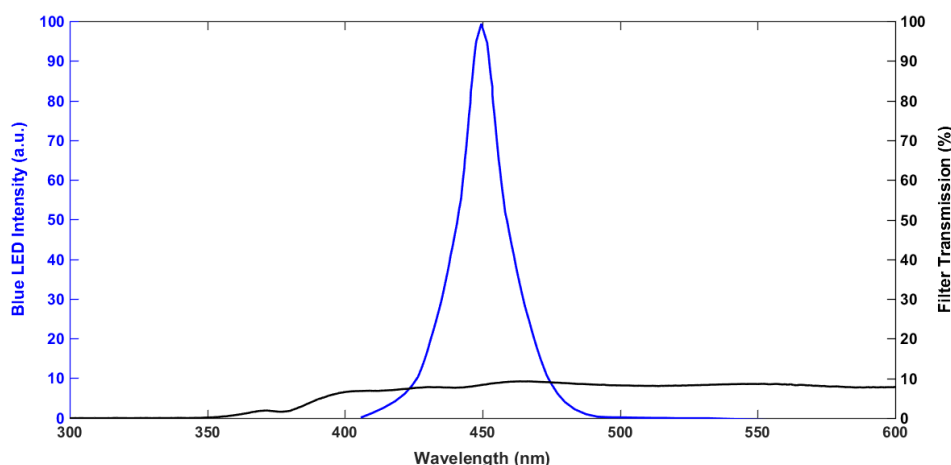


**Figure 3.19** Blue LED illumination intensity profile with maximum intensity at wavelength 450 nm (blue), and transmission spectrum of Neutral Density filter (black)

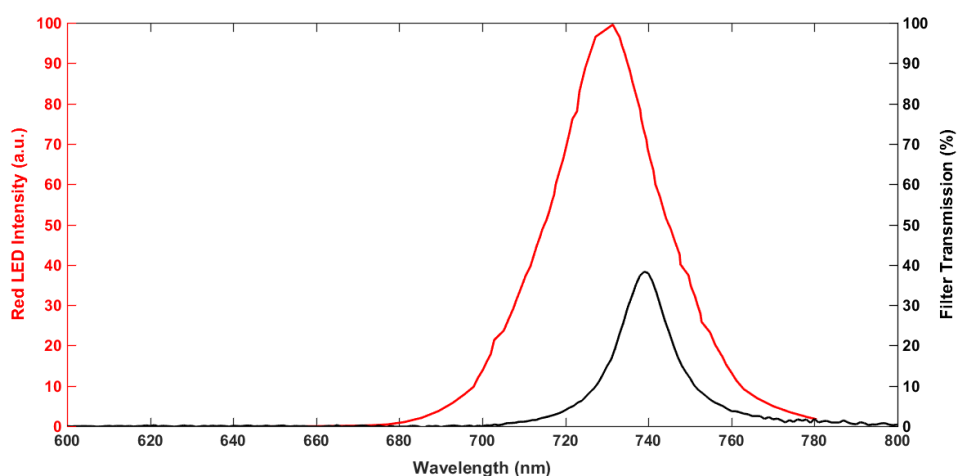


**Figure 3.20** Near infra-red LED illumination intensity profile with maximum intensity at wavelength 730 nm (red), and transmission spectrum of the filter (black).

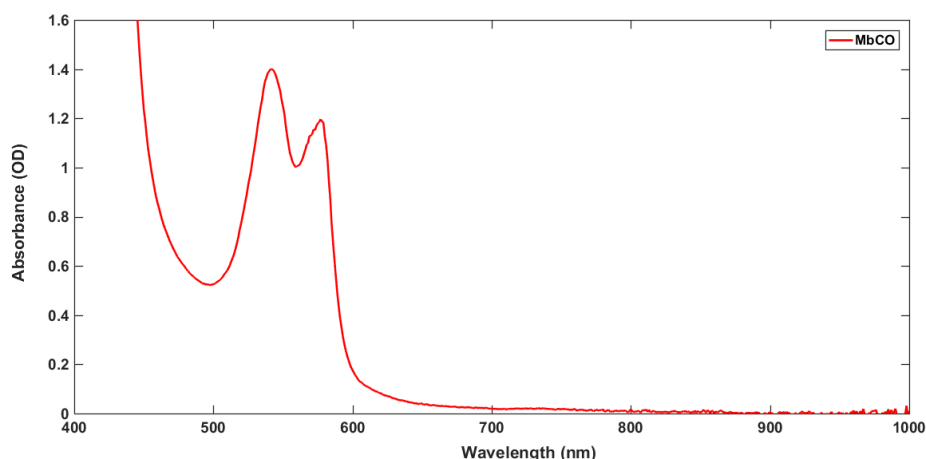


**Figure 3.21** Absorption Spectra of MbCO sample solution

#### 3.2.8 Comparison and calculation of quantum yield efficiency for photodissociation of unlabeled Mb-CO by near infra-red and blue LEDs

The ratio of illumination efficiencies of red to blue was obtained as 16.1. Observing the same effect under both blue and red illumination in our experiment, would indicate a quantum yield for the red illumination of around 6%. Since the illumination of MbCO experiments showed no significant effect for red, the quantum yield in the red has to be in fact be much less than unity.

$$\frac{N_{\text{breaking bond-RED}}}{N_{\text{breaking bond-BLUE}}} = \left( \frac{\eta_0(R)}{\eta_0(B)} \right) \cdot 16.1 \quad 3.2$$

$$\eta_0(R) < 0.06 \eta_0(B)$$

However, the quantum yield of blue LED is 1 ( $\eta_0(B) = 1$ ), so as upper estimation the quantum yield of photodissociation of MbCO with near infra-red LED should be significantly below 1;  $\eta_0(R) < 0.06$ . It should be noted that we should also consider an error for the value of absorbability of MbCO at the wavelength of 730 nm, because the OD at this wavelength is close to the noise of spectrometer at the used concentration in this experiment.

Finally, we could not precisely determine the dissociation quantum yield of MbCO under far red light because of the complicated mixture of products. However, we can have an upper bound quantum yield, it has to be less than 6%.

### 3.3 Conclusion and outlook

Based on the experiment results from the MbCO illumination by the near infra-red LED in the presence of  $H_2O_2$  and comparing to the blue LED illumination results as the reference experiment, we could estimate an upper bound quantum yield of MbCO photodissociation, and it has to be less than 6%.

For an improved estimate of the dissociation yield and to test the possibility to monitor CO binding with red-excited fluorescence, we propose the following experiment, using

MbCO labeled with the red-emitting dye ATTO740. Excitation of this dye provides a much more efficient excitation mechanism of Mb through FRET from the ATTO740 donor. By monitoring the deoxy-Mb and met-Mb produced by dye illumination (still under oxidative conditions to prevent CO rebinding), we will determine the number of dye excitations required to photodissociate MbCO with red light. At the same time, the number of absorbed photons by ATTO740 before dissociation will give us the number of fluorescence photons which we can expect from each labeled MbCO before it gets split by a red excitation. If this number is larger than about 100, the inverse detection yield of our microscope, it will be possible to follow the binding state of Mb in real time at the single-molecule level. Another possible way to improve this experiment to reach better estimation of quantum yield is to use the sample cuvette with a path length of 10 mm for the monitoring beam (as before) and a path length of less than 1 mm (in contrast to before that was 10 mm) for the photolyzing light, which helps to illuminate more efficiently the MbCO molecules in the shorter path as the absorbability of MbCO at 730 nm is small.

## References

- (1) Pradhan, B.; Engelhard, C.; Mulken, S. V.; Miao, X.; Canters, G. W.; Orrit, M. Single Electron Transfer Events and Dynamical Heterogeneity in the Small Protein Azurin from *Pseudomonas Aeruginosa*. *Chem. Sci.* **2020**, *11* (3), 763–771.
- (2) Tabares, L. C.; Gupta, A.; Aartsma, T. J.; Canters, G. W. Tracking Electrons in Biological Macromolecules: From Ensemble to Single Molecule. *Molecules* **2014**, *19* (8), 11660–11678.
- (3) Bowen, W. J. The Absorption Spectra and Extinction Coefficients of Myoglobin. *J. Biol. Chem.* **1949**, *179* (1), 235–245.
- (4) Yusa, K.; Shikama, K. Oxidation of Oxymyoglobin to Metmyoglobin with Hydrogen Peroxide: Involvement of Ferryl Intermediate. *Biochemistry* **1987**, *26* (21), 6684–6688.

